Mol Neurobiol (2012) 45:405–414
DOI 10.1007/s12035-012-8252-2

Effect of Pesticides on the Aggregation of Mutant Huntingtin Protein

Ruhi S. Deshmukh · Rajeev K. Chaudhary · Ipsita Roy

Received: 5 December 2011 / Accepted: 28 February 2012 / Published online: 14 March 2012

Abstract The classical reports on neurodegeneration concentrate on studying disruption of signalling cascades. Although it is now well recognized that misfolding and aggregation of specific proteins are associated with a majority of these diseases, their role in aggravating the symptoms is not so well understood. Huntington's disease (HD) is a neurodegenerative disorder that results from damage to complex II of mitochondria. In this work, we have studied the effect of mitochondrial complex I inhibitors, viz. 1-methyl-4-phenyl-1,2,3,6-tetrahydropyridine and rotenone, and complex II inhibitor, viz. 3-nitropropionic acid, on the aggregation of mutant huntingtin (mthtt) protein, whose misfolding and aggregation results in cellular abnormalities characteristic of HD. All three inhibitors were found to accelerate the aggregation of mthtt in vitro, although the amounts of aggregates formed were different in all cases. Thus, apart from their effect on mitochondrial viability, these neurotoxins are capable of interfering with the protein aggregation process and thus, hastening the onset of the disease.

Keywords Huntingtin · Huntington's disease · Pesticide · Polyglutamine length · Protein fibrillation

Introduction

Numerous epidemiological studies have shown a link between environmental factors and prevalence of neurodegenerative diseases. Increasingly rigorous studies report a direct cause-and-effect relation between environmental agents such as metal ions, infectious agents, pesticides and insecticides, organic solvents, air pollutants, stress, etc. and development of neurological disorders [5, 9, 15, 18, 19, 22, 24, 26, 39, 59, 66, 75]. Parkinson's disease (PD) and Alzheimer's disease (AD) are leading examples of such disorders. Idiopathic PD is increasingly being referred to as an environmental disorder [7, 32, 71]. The development of symptoms is associated with increasing exposure to Cu, Mn or Pb emissions [75]. The association of PD with pesticides is well established. PD-like symptoms had initially been reported in IV-drug users, who injected themselves with mepiridine or synthetic heroin. The causative agent was identified as 1-methyl-4-phenyl-1,2,3,6-tetrahydropyridine (MPTP), a contaminant in the preparation [38]. The exposure of lab animals to pesticides such as rotenone, paraquat, etc. led to depletion of dopaminergic neurons and loss of tyrosine hydroxylase-positive termini, the classical symptoms of parkinsonism [4, 47]. Occupational exposure to solvents such as perchloroethylene, carbon disulphide, methanol, etc. is also associated with parkinsonism. These effects could not be reversed even when the source of exposure was removed [20, 21, 24]. In most of these cases, the causative agents were mitochondrial complex I inhibitors. The hypothesis was that these molecules inactivated mitochondria and resulted in progressive cytotoxicity [11, 14]. However, it has now been shown that metal ions, pesticides, MPTP, etc. can induce aggregation of α-synuclein, the protein implicated in PD, in vitro [30, 69]. Thus, the direct interaction of the neurotoxin with the protein is a matter of concern.

The role of xenobiotic agents in the aggregation of proteins implicated in various monogenic neurological disorders, like Huntington's disease (HD) or familial Parkinson's disease, is less well explored. HD belongs to the class of polyglutamine (polyQ) disorders. The disease is caused by a genetic mutation called CAG repeat expansion in exon 1 of *huntingtin* gene (IT-15) encoding a polyglutamine stretch in the huntingtin protein (Htt) [28]. It is an autosomal dominant disorder in which selective neuronal death occurs primarily in the cortex and

R. S. Deshmukh · R. K. Chaudhary · I. Roy (✉)
Department of Biotechnology, National Institute of Pharmaceutical Education and Research (NIPER),
Sector 67, S.A.S. Nagar,
Punjab 160 062, India
e-mail: ipsita@niper.ac.in

striatum. HD is characterized by personality changes, motor impairment and subcortical dementia. The severity of symptoms is directly proportional to the length of the polyglutamine stretch. However, not all individuals with similar polyQ tract length develop the disease at the same age [53]. This reflects the effect of environment on the progress of the disease. The lack of correlation between phenotype and genotype in some cases of HD, especially monozygotic twins, may provide clues to the role of environment on the onset/progress of monogenic diseases [33]. Similar reports are available for other polyglutamine disorders such as spinocerebellar ataxias [2, 17]. The role of environmental toxins in inducing epigenetic changes has been identified as a major risk factor in the development/progress of the disease in such cases [31]. A recent case study correlating substance abuse and HD reported that controlling for glutamine repeat length in the expanded allele, individuals with histories of alcohol or drug abuse showed a significantly lower age of onset of the disease [8]. A gender bias was also observed with female participants exhibiting an earlier onset of disease when compared with their male counterparts with a similar history of substance abuse. Comparison of striatal proteomes of wild-type and HD(YAC128Q) mice by two dimensional differential gel electrophoresis (DIGE) identified 16 proteins whose expression was altered on exposure to Mn^{2+} in case of HD mice [72]. Most of these proteins were associated with cytoskeletal mobility, glutamatergic neurotransmission and energy metabolism. This suggests that exposure to Mn^{2+}, an environmental toxin, induces toxicity in HD mice by altering the interaction of the mutant huntingtin (128Q) with these proteins, thus affecting various cellular processes.

Unlike α-synuclein, no report is available regarding interaction of mutant huntingtin with environmental agents. In this work, we have studied the effect of mitochondrial complex I inhibitors, rotenone and MPTP, and the complex II inhibitor, 3-nitropropionic acid (3-NP), on the aggregation profile of mutant huntingtin. Exposure to 3-NP, a fungal-derived neurotoxin, has been reported to cause HD-like symptoms in Drosophila, rats and mice [3, 40, 43]. 3-NP is a mitochondrial complex II inhibitor and is increasingly being used to generate HD animal models [43, 67]. Damage to mitochondrial complex II has been shown to be associated with development of HD. We show that both complex I and complex II inhibitors are able to modulate the fibrillation of mutant huntingtin protein.

Materials and Methods

Materials

Isopropyl-1-thio-β-D-galactopyranoside (IPTG), glutathione–agarose matrix, reduced L-glutathione, rotenone, MPTP, 3-NP, ANS (8-anilino-1-naphthalene sulphonic acid), Thioflavin T and Congo red were purchased from Sigma–Aldrich Chemicals Pvt. Ltd., Bangalore, India. The primary antibody (mouse anti polyglutamine) was purchased from Millipore, USA. The secondary antibody (goat anti-mouse HRP conjugated) and TMB/H_2O_2 were purchased from Bangalore Genei Pvt. Ltd., Bangalore, India. The plasmid pGEX-5X1-HD-exon 1-CAG 51 was received as a gift from Prof. E. Wanker (Max-Delbrück-Centrum für Molekulare Medizin (MDC), Berlin, Germany).

Methods

Purification of Mutant Huntingtin Fragment

The plasmid pGEX-5X1-HD-exon 1-CAG 51 was used to transform competent *E. coli* BL21 cells following standard protocol [55]. The transformed cells were inoculated in 2.5 % (*w*/*v*) Luria Bertani medium containing ampicillin (0.006 % *w*/*v*) and grown at 37°C and 200 rpm till an A_{600} of 0.6. Protein expression was induced by the addition of 1 mM IPTG. The expressed protein was purified using glutathione–agarose matrix [57]. The concentration of protein in different fractions was determined by the dye-binding method [6] using bovine serum albumin as the standard protein. The purity of the eluted protein was checked by SDS-PAGE [37] and confirmed by immunoblotting using an anti-polyglutamine antibody as the primary antibody and an anti-mouse HRP conjugated secondary antibody. The purified protein was dialyzed against 0.04 M Tris HCl, pH 8.0 containing 150 mM NaCl and 1 mM EDTA to remove reduced glutathione prior to use.

Aggregation of Mutant Huntingtin Fragment

Mutant huntingtin fragment (mthtt) (0.5 mg ml^{-1}, 0.04 M Tris HCl, pH 8.0) was incubated at 37°C in the presence and absence of pesticides/fungicide. Aliquots were withdrawn at different time intervals and analysed using various biophysical techniques.

ThT Fluorescence Emission Intensity

The protein samples and ThT (in 0.04 M Tris HCl, pH 8.0 containing 150 mM NaCl) were mixed together and the final volume adjusted so as to obtain a molar ratio of 1.5:50, protein to dye. ThT fluorescence emission spectra were recorded at 485 nm after excitation at 440 nm, using a spectrofluorimeter (Shimadzu RF—5301PC). The excitation slit width was kept at 5 nm and that for emission was 10 nm.

The aggregation kinetics was followed by fitting the data using the formula [70],

$$y = y_i + mx_i + \frac{y_f + mx_f}{1 + e^{\frac{x-x_0}{\tau}}}$$

where y_i+mx_i is initial line, y_f+mx_f is the final line and x_0 is the midpoint of maximum signal. The apparent rate constant (k_{app}) is $1/\tau$ and lag time is calculated to be $x_0-2\tau$.

ANS Fluorescence Emission Intensity

The protein samples and 8-anilino-1-naphthalene sulphonic acid (ANS) (in 40 mM Tris HCl, pH 8.0 containing 150 mM NaCl) were mixed together and the final volume adjusted so as to obtain a molar ratio of 1:40, protein to dye. ANS fluorescence emission spectra were recorded at 483 nm after excitation at 360 nm, using a spectrofluorimeter (Shimadzu RF—5301PC) [36].

Congo Red Difference Spectroscopy

A stock solution of Congo red (300 mM) was prepared in 10 % (*v*/*v*) ethanol. The solution was centrifuged at 10,000×*g* for 10 min to remove undissolved dye. The protein samples and Congo red solution were mixed and the final volume adjusted so as to obtain a molar ratio of 2:5, protein to dye. The samples were incubated for 30 min and the Congo red absorbance spectra were recorded between 400 and 700 nm, using a spectrophotometer (Shimadzu UV-1700 PharmaSpec) [46]. The spectrum of Congo red alone was subtracted from the spectra of the corresponding samples containing protein.

SDS-PAGE and Western Blotting

SDS-PAGE (12 % crosslinked polyacrylamide gel) was carried out to analyze aggregates formed after incubation of mthtt under different conditions. Electrophoresis was carried out in miniVE electrophoresis unit (GE Healthcare, Uppsala, Sweden) under conditions of constant voltage. Gels were silver stained. For immunoblotting, proteins bands were transferred electrophoretically to nitrocellulose membranes. Mthtt bands were detected using anti-polyglutamine monoclonal antibody as the primary antibody and goat anti-mouse horseradish peroxidase conjugated antibody as the secondary antibody. Protein bands were visualized using tetramethyl benzinide/hydrogen peroxide (TMB/H_2O_2), which acts as a substrate for horseradish peroxidase.

Results and Discussion

Purification and Aggregation of Mutant Huntingtin Fragment (mthtt)

It has now been conclusively shown that the expression of the first exon of *huntingtin* gene in model systems is sufficient to recapitulate pathology of HD. Proteolytic cleavage of the N-terminal fragment containing the exon I product is responsible for cytotoxicity [23]. Flanking sequences have also been shown to alter the aggregation propensity of the glutamine-rich segment. Expansion of the polyglutamine segment in chimeras resulted in changes in the conformation of the adjacent protein at either of the termini [29]. Using a yeast model, toxicity of polyglutamine segments has been shown to be profoundly altered by flanking sequences [16]. It has recently been shown that the N-terminal 17-amino acid segment upstream of the polyglutamine tract is also able to modulate the aggregation propensity of the protein [65]. It has been proposed that this 17-amino acid stretch may be responsible for the switch of the disordered polyglutamine segment to amyloid fibrils [64].

The target protein (GST-HD51Q) was purified by affinity chromatography. The purity of the eluted protein was checked by denaturing gel electrophoresis (12 % crosslinked polyacrylamide gel) (Fig. 1). Western blotting of samples confirmed the identity of the protein band (Fig. 1).

Mthtt was subjected to aggregation as described in the "Methods" section. The extent of aggregation was monitored by ThT fluorescence spectroscopy. ThT is a cationic benzothiazole dye, which has been reported to show an increased fluorescence upon binding to amyloid fibrils [30, 46, 70]. ThT fluorescence emission spectra were recorded for each of the samples and the emission intensity at 485 nm was plotted against time (Fig. 1). The maximal fluorescence was reached within a short period of time. Such sigmoidal curves, showing nucleation, growth and saturation phases, are characteristic of fibrillation mode of aggregation and have been exhibited by other proteins as well [1, 12, 30, 70]. The lag time of fibrillation was calculated to be 0.61 h and the apparent rate constant of fibrillation was 1.3 h^{-1}. There are diverse views in the literature regarding the manner in which fibrillation proceeds. According to one viewpoint, competition between residual native interactions in the denatured protein and favourable interaction between partially unfolded structures determines the conformation of the final product [1, 61]. A second opinion leans towards the view that crossed β-sheet structures are formed following a complete rearrangement of the native structure [12, 62]. The fluorescence intensity of the hydrophobic dye ANS has been reported to be significantly enhanced upon binding to hydrophobic clusters in proteins [1, 36, 58]. The fluorophore has been used as a reporter dye for the "molten globule" state of the protein. ANS fluorescence

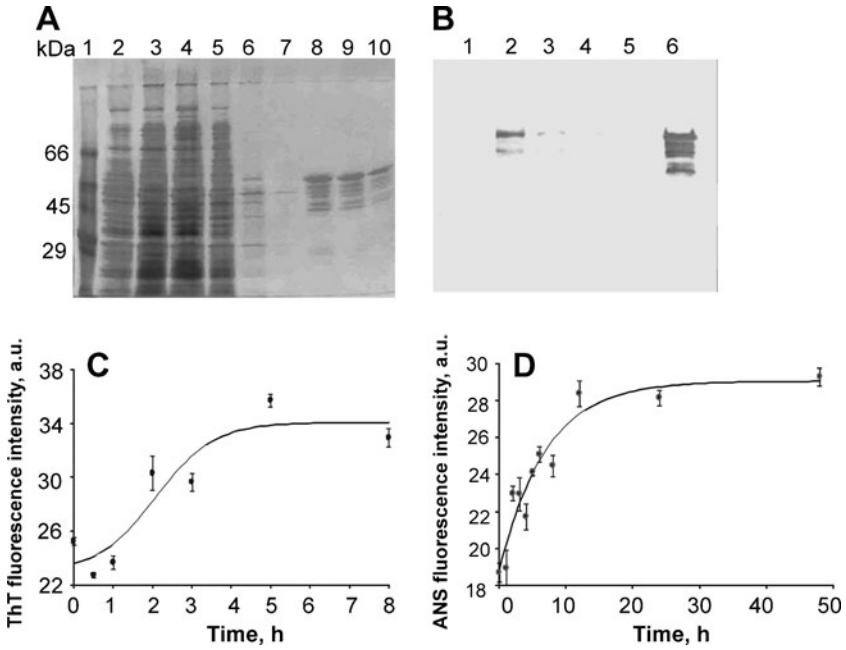

Fig. 1 **A** SDS PAGE (12 % crosslinked polyacrylamide gel) of mutant huntingtin fragment. *Lane 1*: molecular marker, *lane 2*: lysate (uninduced cells), *lane 3*: lysate (induced cells), *lane 4*: flowthrough, *lane 5*: washing 1, *lane 6*: washing 2, *lane 7*: washing 5, *lane 8*: eluate 1, *lane 9*: eluate 2 and *lane 10*: eluate3. The amount of protein loaded in each lane was 20 μg. The gel was silver stained. **B** Western blotting to monitor purification of mutant huntingtin fragment. *Lane 1*: lysate (uninduced cells), *lane 2*: lysate (induced cells), *lane 3*: flowthrough, *lane 4*: washing 1, *lane 5*: washing 5 and *lane 6*: eluate 1. **C** Plot of ThT fluorescence emission intensity against time for aggregation of mthtt incubated at 37°C. **D** Plot of ANS fluorescence emission intensity against time for aggregation of mthtt incubated at 37°C. Experiments were carried out in triplicate and mean±s.d. values are shown

emission spectra were recorded in the presence of protein samples and the emission intensity at 483 nm was plotted against time (Fig. 1). As can be seen, an initial increase in the fluorescence intensity was followed by saturation, indicating that the protein unfolding had been initiated with significant retention in its secondary structure. A comparison of the time-dependent curves for ThT and ANS fluorescence intensities shows that the maximum fluorescence intensity was reached much earlier for Thioflavin T than for ANS. This implies that the formation of the fibrillar structure occurred without a drastic change in the three-dimensional architecture of the protein.

Although still controversial, a major thrust in the therapeutic strategy of HD and other protein misfolding diseases is in the development of screening protocols for aggregation inhibitors. The progressive deposition of aggregates has been associated with the progress of the disease although some other reports consider it to be a cellular defence mechanism. The different stages of aggregation, viz. oligomeric or protofibrillar and polymeric or fibrillar, have been linked to different levels of toxicity [60, 63, 73].While there is a growing viewpoint that amyloid fibril formation may not, in itself, have pathological consequences, the toxicity of different intermediate species is beyond doubt. Addition of Congo red, an anti-amyloid compound, to a suspension of HeLa cells expressing elongated polyglutamine stretch, inhibited ATP depletion even in cases where aggregates had already formed [56]. R6/2 transgenic mice model of HD showed improvement in motor and neurological properties upon infusion of Congo red. This correlated well with reduced appearance of polyglutamine antibody-stained aggregates in basal ganglia of post mortem HD mice [56]. In a recent study with Drosophila HD model, expression of Q138 huntingtin in neurons (mimicking juvenile HD) was accompanied by formation of cytoplasmic and neuritic aggregates and lethality [73]. No mthtt protein was localized in the nucleus and distinct aggregates could be seen in the cytoplasm of neuronal cells and salivary glands (when Q138 is expressed there), and secretion of glue protein Sgs3 was affected. Thus, formation of aggregates may be considered as a marker for the progression of HD.

Effect of MPTP on Aggregation of mthtt

Pesticides and neurotoxins have been shown to interact directly with proteins involved in neurodegenerative diseases in vitro, e.g. α-synuclein, and increase their aggregation in a dose-dependent manner [69]. We have recently shown that MPTP, and not its metabolite MPP^+, is sufficient to induce fibrillation of α-synuclein [30]. The effect of MPTP, a known neurotoxin [45], on the aggregation pattern of mthtt was studied. MPTP (100 μM and 20 mM) was incubated with the protein (0.5 mg ml^{-1}) at 37°C and the aggregation pattern

was monitored by ThT fluorescence spectroscopy (Fig. 2). The plot of emission intensity against time in the presence of 100 μM MPTP showed a sigmoidal curve, indicating nucleation mode of fibrillation. The lag time of fibrillation was 0.13 h, which is less than the lag time for fibrillation of mthtt alone (0.61 h). The apparent rate constant of fibrillation was also higher (7.9 h^{-1}) in the presence of MPTP. At a higher concentration of MPTP (20 mM), fibrillation still occurred, as shown by increased fluorescence of ThT (Fig. 2). However, the non-sigmoidal nature of the curve in this case shows that the mode was not nucleation based. The aggregation pattern of mthtt was also monitored using ANS fluorescence spectroscopy (Fig. 2). Increase in fluorescence intensity of ANS during change in the conformation of a protein is a hallmark of the molten globule state. A comparison of the emission intensity kinetics with ThT showed that in the presence of 100 μM MPTP, nucleus formation preceded formation of the 'molten globule'. The formation of two different substructures agrees well with the recently proposed hypothesis that the molten globule is not a single state but rather a mixture of partially folded units forming oligomers in the kinetic pathway of aggregation [51].

The fibrillar structures formed at the end of the study period were analyzed by a colorimetric assay specific for amyloid fibrils [46]. Mthtt was incubated with Congo red and the difference spectrum of Congo red in the presence and absence of the protein-neurotoxin complex was plotted (Fig. 2). A red shift in the wavelength of maximal absorption of the protein incubated in the absence and presence of MPTP at 37°C as compared with the difference spectrum of mthtt which has not been incubated at 37°C and hence does not form amyloid fibrils, confirmed the amyloid nature of the aggregates in both cases. An increase in the absorbance values at all wavelengths was observed when mthtt aggregates were added to Congo red solution. This was probably due to scattering of light by the aggregates.

The results reported here show a direct interaction between MPTP, a mitochondrial complex I inhibitor and mthtt, resulting in fibrillation of the latter, which is associated with the progress of HD. This may have important implications in the pathogenecity in HD as neurotoxicity due to MPTP exposure has been proven to be responsible for the earlier onset of PD.

Effect of Rotenone on Aggregation of mthtt

Rotenone is a mitochondrial complex I inhibitor and has been used to induce PD-like symptoms in lower animal models [68]. In vitro interaction of rotenone with mthtt was studied by incubating rotenone (100 μM) with the protein at 37°C and monitoring the aggregation kinetics by ThT fluorescence spectroscopy (Fig. 3). A sigmoidal curve was observed, indicating nucleation mode of aggregation. The lag time of fibrillation was 1 h, which was marginally higher than that in the absence of the toxin. However, the apparent rate constant of fibrillation, k_{app} (6.1 h^{-1}), was significantly higher. A plot of change in ANS fluorescence intensity with time (Fig. 3) showed that in case of rotenone-induced aggregation of mthtt, the increase in fluorescence intensity of ThT followed the increase in ANS fluorescence intensity. This implies that the molten globule substructure

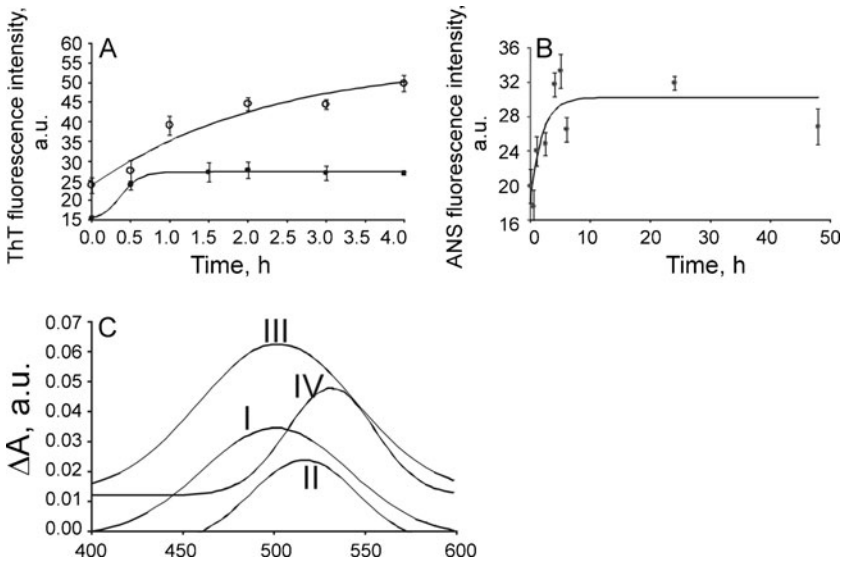

Fig. 2 Aggregation of mthtt in the presence of MPTP. **A** Plot of ThT fluorescence emission intensity against time for aggregation of mthtt incubated in the presence of 100 μM (*filled circle*) and 20 mM (*blank circle*) MPTP at 37°C. **B** Plot of ANS fluorescence emission intensity against time for aggregation of mthtt incubated in the presence of 100 μM MPTP at 37°C. **C** Congo red difference spectroscopy of (*I*) mthtt incubated at 4°C, (*II*) mthtt incubated at 37°C, (*III*) mthtt incubated in the presence of 100 μM MPTP at 37°C and (*IV*) mthtt incubated in the presence of 20 mM MPTP at 37°C. Experiments were carried out in triplicate and mean±s.d. values are shown

is formed before the nucleus for fibrillation has been formed completely. Thus, the mechanism by which rotenone and MPTP, both mitochondrial complex I inhibitors, induce fibril formation of mthtt, is different. In the first case, the molten globule stage is reached before the commencement of nucleation. In the second case, the route is reversed. Similar to the case of MPTP, the fibrillar nature of the aggregates, formed at the end of the incubation period in the presence of rotenone, was also confirmed by Congo red spectroscopy. Aggregated mthtt was incubated with Congo red and the difference spectra of Congo red in the presence and absence of the protein-neurotoxin complex were plotted. A red shift in the wavelength of maximal absorption in the difference spectra of the protein incubated in the absence and presence of rotenone at 37°C as compared with the difference spectrum of mthtt which had not been incubated at 37°C and hence did not form amyloid fibrils (Fig. 3), confirmed the amyloid nature of the aggregates. A higher concentration of rotenone could not be used because of the insolubility of the toxin in the incubation buffer.

Effect of 3-NP on Aggregation of mthtt

Earlier studies have shown the appearance of HD-like symptoms in animal models upon exposure to mitochondrial complex II inhibitors like 3-nitropropionic acid [3, 40, 43, 67]. Mitochondria is associated with both apoptotic and non-apoptotic cell death. The release of cytochrome c from mitochondria initiates a caspase-dependent apoptotic pathway. The loss of mitochondrial membrane potential, on the other hand, is associated with non-apoptotic cell death. When immortalized striatal cells derived from Hdh^{Q111} (mutant) mouse knock-in embryos were treated with 3-NP, greater loss of mitochondrial membrane potential was seen to occur than in normal striatal cells [54]. This could be ameliorated with cyclosporine A (an inhibitor of permeability transition pore) and ruthenium red (an inhibitor of mitochondrial Ca^{2+} uniporter). Interestingly, rotenone, a mitochondrial complex I inhibitor, showed no discriminatory effect between normal and mutant striatal cells [54]. No cytochrome release or caspase activation was observed, pointing to the non-apoptotic mode of cell death. Thus, mutant huntingtin specifically damages the function of mitochondrial complex II. It has been hypothesized that mutant huntingtin affects the transcriptional regulation of genes involved in striatal signaling [42] and those for adenosine A2a and dopamine D2 receptors [41] and impairs the assembly/functioning of one of the four subunits of mitochondrial complex II [25].

The effect of 3-NP was studied by incubating it at concentrations of 100 μM, 10 mM and 20 mM with mthtt at 37°C. The respective plots of ThT fluorescence emission intensity against time (Fig. 4) confirmed nucleation mode of aggregation in all cases. The lag time changed from 0.61 h in the absence of any pesticide to 1.9, 3.6 and 0.45 h in the presence of 100 μM, 10 mM and 20 mM of 3-NP, respectively. The corresponding apparent rate constants of fibrillation (k_{app}) were 1.2, 1.8 and 4.4 h^{-1}. Since reduction in lag time and increase in k_{app} were observed in case of 20 mM 3-NP, this condition was analyzed further. A plot of ANS fluorescence emission intensity against time, in the presence of 20 mM 3-NP, followed a sigmodal pattern (Fig. 4). The lag time was delayed in this case as compared with the change in fluorescence intensity of ThT, showing that the molten globule state was reached after the fibrillation nucleus had formed. Congo red difference spectrum showed a red shift for the protein

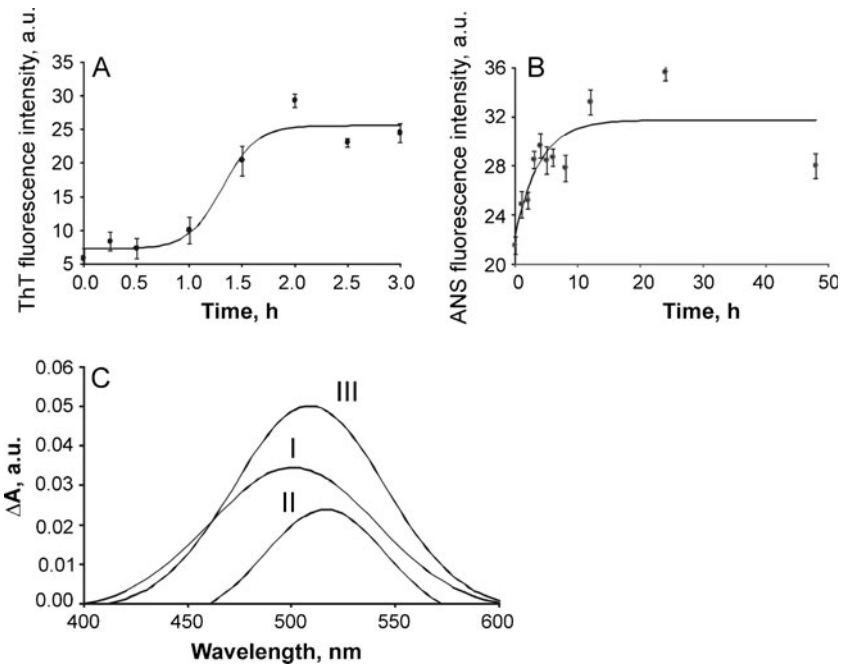

Fig. 3 Aggregation of mthtt in the presence of rotenone. **A** Plot of ThT fluorescence emission intensity against time for aggregation of mthtt incubated in the presence of 100 μM rotenone at 37°C. **B** Plot of ANS fluorescence emission intensity against time for aggregation of mthtt incubated in the presence of 100 μM rotenone at 37°C. **C** Congo red difference spectroscopy of (*I*) mthtt incubated at 4°C, (*II*) mthtt incubated at 37°C and (*III*) mthtt incubated in the presence of 100 μM rotenone at 37°C. Experiments were carried out in triplicate and mean±s.d. values are shown

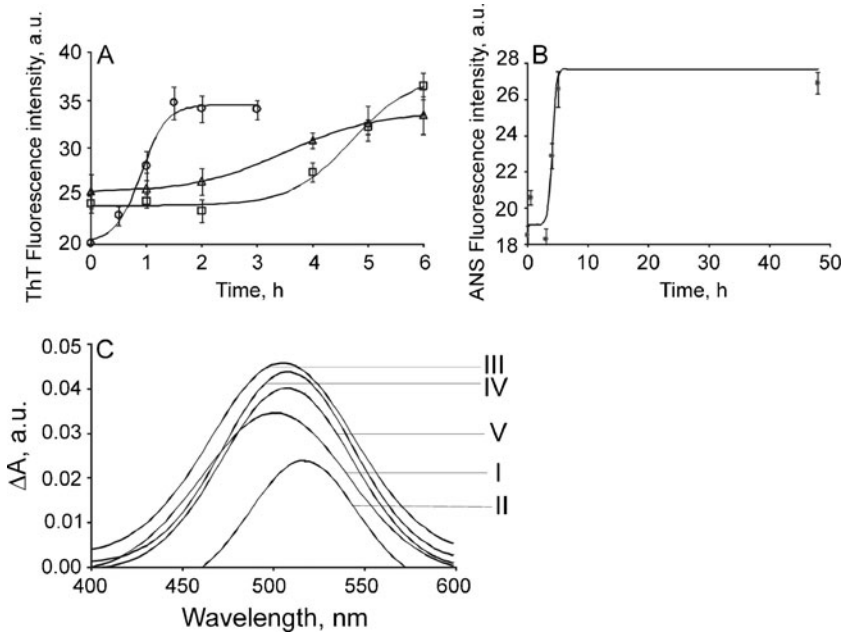

Fig. 4 Aggregation of mthtt in the presence of 3-NP. **A** Plot of ThT fluorescence emission intensity against time for aggregation of mthtt incubated in the presence of 100 μM (*blank triangle*), 10 mM (*blank square*) and 20 mM (*blank circle*) 3-NP at 37°C. **B** Plot of ANS fluorescence emission intensity against time for aggregation of mthtt incubated in the presence of 20 mM 3-NP at 37°C. **C** Congo red difference spectroscopy of (*I*) mthtt incubated at 4°C, (*II*) mthtt incubated at 37°C, (*III*) mthtt incubated in the presence of 100 μM 3-NP at 37°C, (*IV*) mthtt incubated in the presence of 10 mM 3-NP at 37°C and (*V*) mthtt incubated in the presence of 20 mM 3-NP at 37°C. Experiments were carried out in triplicate and mean±s.d. values are shown

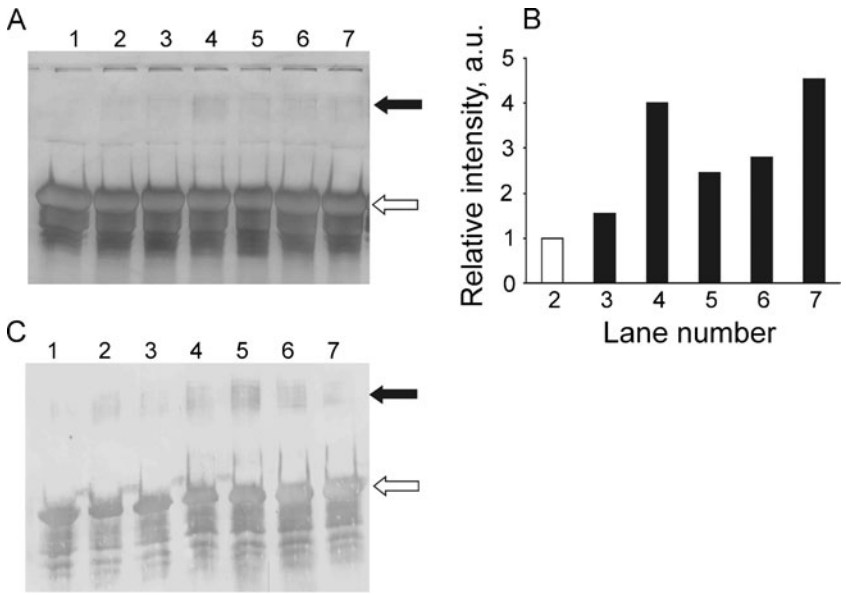

Fig. 5 Analysis of mthtt aggregates. A. SDS-PAGE of aggregated mthtt. *Lane 1*: mthtt at 4°C, *lane 2*: mthtt incubated at 37°C, *lane 3*: mthtt incubated in the presence of 100 μM 3-NP at 37°C, *lane 4*: mthtt incubated in the presence of 10 mM 3-NP at 37°C, *lane 5*: mthtt incubated in the presence of 20 mM 3-NP at 37°C, *lane 6*: mthtt incubated in the presence of 100 μM MPTP at 37°C and *lane 7*: mthtt incubated in the presence of 20 mM MPTP at 37°C. The amount of protein loaded in each lane was 20 μg. **B** Densitometric analysis of aggregates formed following incubation of mthtt alone (*empty bar*) or in the presence of pesticides (*filled bars*). The intensities of the bands were quantified by Image Quant software (GE Healthcare, Uppsala, Sweden) The intensity of the band corresponding to the aggregates formed by mthtt alone has been assigned an arbitrary value of 1. The intensities of all other bands have been calculated with reference to this value. **C** Immunoblotting of aggregated mthtt. *Lane 1*: mthtt at 4°C, *lane 2*: mthtt incubated at 37°C, *lane 3*: mthtt incubated in the presence of 100 μM 3-NP at 37°C, *lane 4*: mthtt incubated in the presence of 10 mM 3-NP at 37°C, *lane 5*: mthtt incubated in the presence of 20 mM 3-NP at 37°C, *lane 6*: mthtt incubated in the presence of 100 μM MPTP at 37°C and *lane 7*: mthtt incubated in the presence of 20 mM MPTP at 37°C. The position of the band for the monomeric protein is indicated by an *empty arrow* while the position of the band for the aggregated protein is indicated by a *filled arrow*

incubated in the absence and presence of 3-NP as compared with the difference spectrum of mthtt which has not been incubated at 37°C (Fig. 4). This confirmed the amyloid nature of the aggregates formed.

Analysis of Aggregates

Electrophoretic analysis of the protein samples incubated in the presence and absence of neurotoxins was carried out by SDS-PAGE (Fig. 5). Aggregates formed via amyloid fibrils have been shown to be SDS-resistant [10, 30, 57, 64]. Densitometric analysis of the bands was carried out using ImageQuant TL® software (GE Healthcare). The amount of aggregates formed was the highest in the case of 10 mM 3-NP and 20 mM MPTP (Fig. 5). The results correlate well with ThT fluorescence intensity data obtained with the aggregated protein. The amount of aggregates formed in the presence of these two neurotoxins was also more as reflected by the relative intensities of the bands in these two cases. These results were confirmed by Western blotting using anti polyglutamine monoclonal antibody as the primary antibody (Fig. 5).

It is interesting to speculate on the possibility of the results obtained here being translated to in vivo systems, especially since HD is largely a monogenic disease. Apart from its effect on degeneration of the central nervous system, 3-NP has recently been shown to have damaging effect on peripheral musculature [27]. This has again been attributed to its deleterious effect on oxidative metabolism. The origin and progress of HD have multifarious reasons. This is clear from the effects of agents as varied as COX inhibitors like Licofelone [34], antioxidants like sesamol [35], PPARγ ligands like pioglitazone [44], antidepressants like sildenafil, etc. [52], on ameliorating 3-NP-induced HD-like changes in cell and animal models. The fact that the neurotoxins can interact directly with the proteins (mthtt in this case) and induce fibrillation shows that therapeutic strategies which concentrate on inhibiting fibrillation will hold some promise for patients of this devastating disease.

Correlation between environmental and genetic factors has also been seen in case of familial PD wherein mutations in α-synuclein (A53T, A30P) have been associated with hereditary forms of the disease. Male transgenic mice expressing mutated α-synuclein (A53T) have been shown to be more susceptible to exposure to the pesticide paraquat [49]. This effect was exacerbated with enhanced oral intake of carbonyl iron in case of neonatal mice (10–17 days), followed by intraperitoneal injection of the pesticide, as measured by the loss in tyrosine hydroxylase positive neurons. Administration of paraquat alone or in combination with iron has earlier been shown to increase the levels of 3-nitrotyrosne oxidation in dopaminergic neurons [50]. Systemic administration of an antioxidant (EUK-189) was found to attenuate the loss of dopaminergic neurons, either pre- or postexposure to iron-paraquat [49]. Thus, it is possible that exposure to environmental toxins, like paraquat or iron, leads to modifications in the protein (α-synuclein), which aids free radical-mediated oxidative damage to dopaminergic neurons and accelerates the progress of the disease. The earlier hypothesis that the neurotoxin MPTP needs to be converted to MPP^+ to exhibit its neurodegenerative effect is partially nullified by the observations that MPTP alone can induce aggregation of α-synuclein [30] and that Ndufs4-deleted mice (which cannot assemble complete mitochondrial complex I) exhibit the same level of sensitivity to MPP^+ as wild type mice [13]. Thus, the observation that the aggregation of mutant huntingtin can be accelerated in the presence of neurotoxins may have important implications for individuals where the polyglutamine stretch is of intermediate length (39–60) and where a slow disease progression would have been anticipated otherwise.

Conclusion

The in vitro experiments described above show that 3-NP, a known inhibitor of succinate dehydrogenase in mitochondrial complex II, is able to initiate fibrillation of mthtt. What is interesting and even more important is that MPTP, a mitochondrial complex I inhibitor, accelerates the fibrillation of mthtt. MPTP has been identified as a mitochondrial complex I inhibitor whereas HD is associated with damage to mitochondrial complex II. MPTP is associated with the development of PD, but as far as we are aware, it has not been implicated in HD. In view of the sporadic reports that damage to mitochondrial complex I is also associated with HD, although not to the same extent as mitochondrial complex II [48, 74], the effect of both neurotoxins in HD needs to be studied in greater detail. This study should not be limited to the effect of the neurotoxins on the inactivation of mitochondria but also include the direct modulation of aggregation of mutant huntingtin by it.

Acknowledgments The authors are thankful to Department of Science and Technology and Department of Biotechnology (Government of India organizations) for partial financial support. RKC acknowledges the award of senior research fellowship by Indian Council of Medical Research (Government of India). The funding agencies had no role in the study design, collection, interpretation or analysis of data, in the writing of the report and in the decision to submit the paper for publication.

References

1. Ahmad B, Winkelmann J, Tiribilli B, Chiti F (2010) Searching for conditions to form stable protein oligomers with amyloid-like characteristics: the unexplored basic pH. Biochim Biophys Acta 1804:223–234
2. Anderson JH, Christova PS, Xie TD, Schott KS, Ward K, Gomez CM (2002) Spinocerebellar ataxia in monozygotic twins. Arch Neurol 59:1945–1951
3. Beal MF, Brouillet E, Jenkins BG, Ferrante RJ, Kowall NW, Miller JM, Storey E, Srivastava R, Rosen BR, Hyman BT (1993)

Neurochemical and histologic characterization of striatal excitotoxic lesions produced by the mitochondrial toxin 3-nitropropionic acid. J Neurosci 13:4181–4192
4. Berry C, La Vecchia C, Nicotera P (2010) Paraquat and Parkinson's disease. Cell Death Differ 17:1115–1125
5. Block ML, Calderon-Garciduenas L (2009) Air pollution: mechanisms of neuroinflammation and CNS disease. Trends Neurosci 32:506–516
6. Bradford MM (1976) A rapid and sensitive method for the quantitation of microgram quantities of protein utilizing the principle of protein-dye binding. Anal Biochem 72:248–254
7. Burbulla LF, Krüger R (2011) Converging environmental and genetic pathways in the pathogenesis of Parkinson's disease. J Neurol Sci 306:1–8
8. Byars JA, Beglinger LJ, Moser DJ, Gonzalez-Alegre P, Nopoulos P (2012) Substance abuse may be a risk factor for earlier onset of Huntington disease. J Neurol. doi:10.1007/s00415-012-6415-8
9. Campbell A (2002) The potential role of aluminium in Alzheimer's disease. Nephrol Dial Transplant 17:17–20
10. Cappai R, Leck SL, Tew DJ, Williamson NA, Smith DP, Galatis D, Sharples RA, Curtain CC, Ali FE, Cherny RA, Culvenor JG, Bottomley SP, Masters CL, Barnham KJ, Hill AF (2005) Dopamine promotes alpha-synuclein aggregation into SDS-resistant soluble oligomers via a distinct folding pathway. FASEB J 19: 1377–1379
11. Castello PR, Drechsel DA, Patel M (2007) Mitochondria are a major source of paraquat-induced reactive oxygen species production in the brain. J Biol Chem 282:14186–14193
12. Chiti F, Bucciantini M, Capanni C, Taddei N, Dobson CM, Stefani M (2001) Solution conditions can promote formation of either amyloid protofilaments or mature fibrils from the HypF N-terminal domain. Protein Sci 10:2541–2547
13. Choi W-S, Kruse SE, Palmiter RD, Xia Z (2008) Mitochondrial complex I inhibition is not required for dopaminergic neuron death induced by rotenone, MPP^+, or paraquat. Proc Natl Acad Sci USA 105:15136–15141
14. Choi WS, Palmiter RD, Xia Z (2011) Loss of mitochondrial complex I activity potentiates dopamine neuron death induced by microtubule dysfunction in a Parkinson's disease model. Cell Biol 192:873–882
15. Corrigan FM, Wienburg CL, Shore RF, Daniel SE, Mann D (2000) Organochlorine insecticides in substantia nigra in Parkinson's disease. J Toxicol Environ Health A 59:229–234
16. Duennwald ML, Jagadish S, Muchowski PJ, Lindquist S (2006) Flanking sequences profoundly alter polyglutamine toxicity in yeast. Proc Natl Acad Sci USA 103:11045–11050
17. Durr A (2010) Autosomal dominant cerebellar ataxias: polyglutamine expansions and beyond. Lancet Neurol 9:885–894
18. Ferreira PC, Tonani KA, Julião FC, Cupo P, Domingo JL, Segura-Muñoz SI (2009) Aluminum concentrations in water of elderly people's houses and retirement homes and its relation with elderly health. Bull Environ Contam Toxicol 83:565–569
19. Floyd RA, Hensley K (2002) Oxidative stress in brain aging. Implications for therapeutics of neurodegenerative diseases. Neurobiol Aging 23:795–807
20. Gash DM, Rutland K, Hudson NL, Sullivan PG, Bing G, Cass WA, Pandya JD, Liu M, Choi DY, Hunter RL, Gerhardt GA, Smith CD, Slevin JT, Prince TS (2008) Trichloroethylene: Parkinsonism and complex 1 mitochondrial neurotoxicity. Ann Neurol 63:184–192
21. Goldman SM (2010) Trichloroethylene and Parkinson's disease: dissolving the puzzle. Expert Rev Neurother 10:835–837
22. González-Duarte A, Magaña Zamora L, Cantú Brito C, García-Ramos G (2010) Hypothalamic abnormalities and Parkinsonism associated with H1N1 influenza infection. J Neuroinflammation 7:47
23. Graham RK, Deng Y, Slow EJ, Haigh B, Bissada N, Lu G, Pearson J, Shehadeh J, Bertram L, Murphy Z, Warby SC, Doty CN, Roy S, Wellington CL, Leavitt BR, Raymond LA, Nicholson DW, Hayden MR (2006) Cleavage at the caspase-6 site is required for neuronal dysfunction and degeneration due to mutant huntingtin. Cell 125:1179–1191
24. Hageman G, van der Hoek J, van Hout M, van der Laan G, Steur EJ, de Bruin W et al (1999) Parkinsonism, pyramidal signs, polyneuropathy, and cognitive decline after long-term occupational solvent exposure. J Neurol 246:198–206
25. Hägerhäll C (1997) Succinate: quinone oxidoreductases: variations on a conserved theme. Biochim Biophys Acta 1320:107–141
26. Hancock DB, Martin ER, Mayhew GM, Stajich JM, Jewett R, Stacy MA et al (2008) Pesticide exposure and risk of Parkinson's disease: a family-based case-control study. BMC Neurol 8:6
27. Hernandez-Echeagaray E, Gonzalez N, Ruelas A, Mendoza E, Rodríguez-Martínez E, Antuna-Bizarro R (2011) Low doses of 3-nitropropionic acid in vivo induce damage in mouse skeletal muscle. Neurol Sci 32:241–254
28. Huntington Collaborative Research Group (1993) A novel gene containing a trinucleotide repeat that is expanded and unstable on Huntington's disease chromosomes. Cell 72:971–983
29. Ignatova Z, Gierasch LM (2006) Extended polyglutamine tracts cause aggregation and structural perturbation of an adjacent beta barrel protein. J Biol Chem 281:12959–12967
30. Jethva PN, Kardani JR, Roy I (2011) Modulation of α-synuclein aggregation by dopamine in the presence of MPTP and its metabolite. FEBS J 278:1688–1698
31. Kell DB (2010) Towards a unifying, systems biology understanding of large-scale cellular death and destruction caused by poorly liganded iron: Parkinson's, Huntington's, Alzheimer's, prions, bactericides, chemical toxicology and others as examples. Arch Toxicol 84:825–889
32. Kenborg L, Lassen CF, Ritz B, Schernhammer ES, Hansen J, Gatto NM et al (2011) Outdoor work and risk for Parkinson's disease: a population-based case-control study. Occup Environ Med 68:273–278
33. Ketelaar M, Hofstra R, Hayden M (2011) What monozygotic twins discordant for phenotype illustrate about mechanisms influencing genetic forms of neurodegeneration. Clin Genet. doi:10.1111/j.1399-0004.2011.01795.x
34. Kumar P, Kalonia H, Kumar A (2011) Role of LOX/COX pathways in 3-nitropropionic acid-induced HD like symptoms in rats: protective role of Licofelone. Br J Pharmacol 164:644–654
35. Kumar P, Kalonia H, Kumar A (2010) Protective effect of sesamol against 3-nitropropionic acid-induced cognitive dysfunction and altered glutathione redox balance in rats. Basic Clin Pharmacol Toxicol 107:577–582
36. Kundu B, Guptasarma P (2002) Use of a hydrophobic dye to indirectly probe the structural organization and conformational plasticity of molecules in amorphous aggregates of carbonic anhydrase. Biochem Biophys Res Commun 293:572–577
37. Laemmli UK (1970) Cleavage of structural proteins during the assembly of the head of bacteriophage T4. Nature 227:680–685
38. Langston JW, Ballard P, Tetrud JW, Irwin I (1983) Chronic Parkinsonism in humans due to a product of meperidine-analog synthesis. Science 219:979–980
39. Ling Z, Zhu Y, Tong CW, Snyder JA, Lipton JW, Carvey PM (2009) Prenatal lipopolysaccharide does not accelerate progressive dopamine neuron loss in the rat as a result of normal aging. Exp Neurol 216:312–320
40. Ludolph AC, He F, Spencer PS, Hammerstad J, Sabri M (1991) 3-Nitropropionic acid-exogenous animal neurotoxin and possible human striatal toxin. Can J Neurol Sci 18:492–498
41. Luthi-Carter R, Hanson SA, Strand AD, Bergstrom DA, Chun W, Peters NL et al (2002) Dysregulation of gene expression in the R6/

2 model of polyglutamine disease: parallel changes in muscle and brain. Hum Mol Genet 11:1911–1926
42. Luthi-Carter R, Strand A, Peters NL, Solano SM, Hollingsworth ZR, Menon AS et al (2000) Decreased expression of striatal signaling genes in a mouse model of Huntington's disease. Hum Mol Genet 9:1259–1271
43. McConoughey SJ, Basso M, Niatsetskaya ZV, Sleiman SF, Smirnova NA, Langley BC et al (2010) Inhibition of transglutaminase 2 mitigates transcriptional dysregulation in models of Huntington disease. EMBO Mol Med 2:349–370
44. Napolitano M, Costa L, Palermo R, Giovenco A, Vacca A, Gulino A (2011) Protective effect of pioglitazone, a PPARγ ligand, in a 3-nitropropionic acid model of Huntington's disease. Brain Res Bull 85:231–237
45. Natale G, Kastsiushenka O, Fulceri F, Ruggieri S, Paparelli A, Fornai F (2010) MPTP-induced parkinsonism extends to a subclass of TH-positive neurons in the gut. Brain Res 1355:195–206
46. Nilsson MR (2004) Techniques to study amyloid fibril formation in vitro. Methods 34:151–160
47. Pan-Montojo F, Anichtchik O, Dening Y, Knels L, Pursche S, Jung R et al (2010) Progression of Parkinson's disease pathology is reproduced by intragastric administration of rotenone in mice. PLoS One 5:e8762
48. Pandey M, Varghese M, Sindhu KM, Sreetama S, Navneet AK, Mohanakumar KP et al (2008) Mitochondrial NAD^+-linked State 3 respiration and complex-I activity are compromised in the cerebral cortex of 3-nitropropionic acid-induced rat model of Huntington's disease. J Neurochem 104:420–434
49. Peng J, Oo ML, Andersen JK (2010) Synergistic effects of environmental risk factors and gene mutations in Parkinson's disease accelerate age-related neurodegeneration. J Neurochem 115:1363–1373
50. Peng J, Peng L, Stevenson FF, Doctrow SR, Andersen JK (2007) Iron and paraquat as synergistic environmental risk factors in sporadic Parkinson's disease accelerate age-related neurodegeneration. J Neurosci 27:6914–6922
51. Povarova OI, Kuznetsova IM, Turoverov KK (2010) Differences in the pathways of proteins unfolding induced by urea and guanidine hydrochloride: molten globule state and aggregates. PLoS One 5:e15035
52. Puerta E, Hervias I, Barros-Minones L, Jordan J, Ricobaraza A, Cuadrado-Tejedor M et al (2010) Sildenafil protects against 3-nitropropionic acid neurotoxicity through the modulation of calpain, CREB, and BDNF. Neurobiol Dis 38:237–245
53. Rosenblatt A, Brinkman RR, Liang KY, Almqvist EW, Margolis RL, Huang CY, Sherr M, Franz ML, Abbott MH, Hayden MR, Ross CA (2001) Familial influence on age of onset among siblings with Huntington disease. Am J Med Genet 105:399–403
54. Ruan Q, Lesort M, MacDonald ME, Johnson GV (2004) Striatal cells from mutant huntingtin knock-in mice are selectively vulnerable to mitochondrial complex II inhibitor-induced cell death through a non-apoptotic pathway. Hum Mol Genet 13:669–681
55. Sambrook J, Russell DW (2001) Molecular cloning: a laboratory manual, 3rd edn. CSHL press, New York
56. Sánchez I, Mahlke C, Yuan J (2003) Pivotal role of oligomerization in expanded polyglutamine neurodegenerative disorders. Nature 421:373–379
57. Scherzinger ER, Lurz M, Turmaine L, Mangiarini B, Hollenbach R, Hasenbank GP et al (1997) Huntingtin-encoded polyglutamine expansions form amyloid-like protein aggregates in vitro and in vivo. Cell 90:549–558
58. Semisotnov GV, Rodionova NA, Razgulyaev OI, Uversky VN, Gripas AF, Gilmanshin RI (1991) Study of the "molten globule" intermediate state in protein folding by a hydrophobic fluorescent probe. Biopolymers 31:119–128
59. Sparks DL, Schreurs BG (2003) Trace amounts of copper in water induce beta-amyloid plaques and learning deficits in a rabbit model of Alzheimer's disease. Proc Natl Acad Sci USA 100:11065–11069
60. Stefani M (2004) Protein misfolding and aggregation: new examples in medicine and biology of the dark side of the protein world. Biochim Biophys Acta 1739:5–25
61. Taddei N, Chiti F, Fiaschi T, Bucciantini M, Capanni C, Stefani M et al (2000) Stabilisation of alpha-helices by site-directed mutagenesis reveals the importance of secondary structure in the transition state for acylphosphatase folding. J Mol Biol 300:633–647
62. Taddei N, Capanni C, Chiti F, Stefani M, Dobson CM, Ramponi G (2001) Folding and aggregation are selectively influenced by the conformational preferences of the alpha-helices of muscle acylphosphatase. J Biol Chem 276:37149–37154
63. Takahashi T, Kikuchi S, Katada S, Nagai Y, Nishizawa M, Onodera O (2008) Soluble polyglutamine oligomers formed prior to inclusion body formation are cytotoxic. Hum Mol Genet 17: 345–356
64. Tam S, Spiess C, Auyeung W, Joachimiak L, Chen B, Poirier MA, Frydman J (2009) The chaperonin TRiC blocks a huntingtin sequence element that promotes the conformational switch to aggregation. Nat Struct Mol Biol 16:1279–1285
65. Thakur AK, Jayaraman M, Mishra R, Thakur M, Chellgren VM, Byeon IJ, Anjum DH, Kodali R, Creamer TP, Conway JF, Gronenborn AM, Wetzel R (2009) Polyglutamine disruption of the huntingtin exon 1 N terminus triggers a complex aggregation mechanism. Nat Struct Mol Biol 16:380–389
66. Thiruchelvam M, Richfield EK, Baggs RB, Tank AW, Cory-Slechta DA (2000) The nigrostriatal dopaminergic system as a preferential target of repeated exposures to combined paraquat and maneb: implications for Parkinson's disease. J Neurosci 20: 9207–9214
67. Túnez I, Drucker-Colín R, Jimena I, Medina FJ, Muñoz Mdel C, Peña J et al (2006) Transcranial magnetic stimulation attenuates cell loss and oxidative damage in the striatum induced in the 3-nitropropionic model of Huntington's disease. J Neurochem 97:619–630
68. Uversky VN (2004) Neurotoxicant-induced animal models of Parkinson's disease: understanding the role of rotenone, maneb and paraquat in neurodegeneration. Cell Tissue Res 318:225–241
69. Uversky VN, Li J, Bower K, Fink AL (2002) Synergistic effects of pesticides and metals on the fibrillation of alpha-synuclein: implications for Parkinson's disease. Neurotoxicology 23:527–536
70. Uversky VN, Li J, Fink AL (2001) Evidence for a partially folded intermediate in α-synuclein fibril formation. J Biol Chem 276: 10737–10744
71. Vance JM, Ali S, Bradley WG, Singer C, Di Monte DA (2010) Gene-environment interactions in Parkinson's disease and other forms of parkinsonism. Neurotoxicology 31:598–602
72. Wegrzynowicz M, Holt HK, Friedman DB, Bowman AB (2012) Changes in the striatal proteome of YAC128Q mice exhibit gene-environment interactions between mutant huntingtin and manganese. J Proteome Res 11:1118–1132
73. Weiss KR, Kimura Y, Lee WC, Littleton JT (2011) Huntingtin aggregation kinetics and their pathological role in a Drosophila Huntington's disease model. Genetics. doi:10.1534/genetics.111.133710
74. Weydt P, Pineda VV, Torrence AE, Libby RT, Satterfield TF, Lazarowski ER et al (2006) Thermoregulatory and metabolic defects in Huntington's disease transgenic mice implicate PGC-1alpha in Huntington's disease neurodegeneration. Cell Metab 4:349–362
75. Willis AW, Evanoff BA, Lian M, Galarza A, Wegrzyn A, Schootman M (2010) Metal emissions and urban incident Parkinson disease: a community health study of Medicare beneficiaries by using geographic information systems. Am J Epidemiol 172:1357–1363